Cement & Concrete Composites 45 (2014) 46–56

Contents lists available at ScienceDirect

Cement & Concrete Composites

journal homepage: www.elsevier.com/locate/cemconcomp

# Microstructure, strength, and moisture stability of alkali activated glass powder-based binders

Rachel Redden [a], Narayanan Neithalath [b,*]

[a] TRC Engineering and Consulting, 215 Greenfield Parkway, Liverpool, NY, United States
[b] School of Sustainable Engineering and the Built Environment, Arizona State University, Tempe, AZ 85287-5306, United States

ARTICLE INFO

*Article history:*
Received 24 April 2012
Received in revised form 30 July 2013
Accepted 15 September 2013
Available online 23 September 2013

*Keywords:*
Alkali activation
Glass powder
Fly ash
Binder
FTIR spectroscopy
Microstructure

ABSTRACT

Thermally assisted alkali activation of silica-rich glass powder to produce sustainable binders is investigated. Glass powder activated using NaOH provides higher compressive strengths than NaOH activated fly ash binders at lower heat curing temperatures. Sodium silicate gel is the reaction product when glass powder alone is used as the source material, while a combination of sodium silicate and sodium aluminosilicate (N–A–S–H) gels form in activated glass powder–fly ash blends. The activated glass powder-containing binders are found to disintegrate and lose strength when exposed to moisture or an alkaline solution, with the pure glass powder binders suffering the highest strength loss. Structural changes to the reaction product on exposure to moisture are explained using microstructural and FTIR spectroscopic observations. Doping the systems with Al containing (metakaolin) and Ca containing (slag) source materials, while retaining glass powder as the major component (50% or more), result in the formation of moisture-stable reaction products thereby mitigating the strength loss to a large extent.

## 1. Introduction

Alkaline activation of aluminosilicate materials such as fly ash, ground granulated blast furnace slag, and metakaolin has been shown to be capable of producing sustainable binders to replace ordinary Portland cement. The use of these natural or industrial by-product materials results in significant environmental benefits such as the decrease in $CO_2$ emission and energy consumption attributed to Portland cement production, and the conservation of non-replenishable natural resources [1–4]. In addition, this approach allows for increased utilization of materials like fly ash, the management of which is a concern.

Among the source materials used to produce alkali activated concretes, fly ash and slag are the most commonly studied because of their abundant availability and the presence of soluble silica and alumina contents in these materials that undergo dissolution, polymerization with the alkali, and solidification that provides strength and stability to these matrices [5–10]. Alkali hydroxides or silicates of varying concentrations are generally used as the activating agents. The processing conditions required to produce binders of desirable mechanical and durability properties change with the source material chemistry. For instance, activated fly ash binders require mild to moderate thermal curing in order to facilitate hardening and the formation of the alkali aluminosilicate binder [4,7,11] whereas activated slag binders harden and develop strength under moist curing [10,12]. Several studies have reported the reaction product formation and property development in such mixtures [13–17], aiding in a better understanding of these binder systems.

While significant progress is being made on increased utilization of industrial waste materials such as fly ash and slag through alkali activation, there are materials from other waste streams that have the potential to be activated to form sustainable binders. Powdered glass is one such material, which is the focus of this paper. Municipal waste streams across the world generate millions of tons of glass every year. In the United States alone, 12 million tons of waste glass is generated annually, with only a quarter of it being recycled [18]. Fine glass powder has been reported to have adequate pozzolanic properties [19,20] and concretes made with partial replacement of cement by glass powder has shown comparable performance to that of fly ash modified concretes [21,22].

Glass powder is rich in silica, and when activated with alkalis, can result in the formation of sodium silicate gel. Only limited preliminary studies have been reported on alkali activation of glass powder. Limited mechanical properties of activated slag-glass powder mixtures have been evaluated, and is reported that increasing the glass powder content decreases the strength under moist curing conditions [23]. There is a need to understand the reaction product formation in binders that contain glass powder as a major component, and their properties so as to enable

---

* Corresponding author. Tel.: +1 480 965 6023; fax: +1 480 965 0557.
*E-mail addresses:* RRedden@trcsolutions.com (R. Redden), Narayanan.Neithalath@asu.edu (N. Neithalath).

0958-9465/$ - see front matter © 2013 Elsevier Ltd. All rights reserved.
http://dx.doi.org/10.1016/j.cemconcomp.2013.09.011

beneficial utilization of this material. The alkali silicate gels, when exposed to water, can leach alkali ions [24] that contribute to the destabilization of the gel structure. This is an important criterion that needs to be studied with respect to the durability of the activated glass powder binders. This paper evaluates the strength development in NaOH activated glass powder (~72% $SiO_2$) mixtures, and compares the reaction products formed to those found in activated fly ash mixtures. The hydrolytic stability of the reaction products formed from glass powder activation is investigated and methods to produce water-resistant gels containing a major proportion of glass powder are outlined.

## 2. Experimental program

The glass powder used in this study is a by-product of industrial and highway safety glass bead manufacturing, with pozzolanic properties as reported earlier [19,21]. The manufacturing process produces the fine powder as a waste, necessitating no grinding or pre-treatment before the glass powder can be used as a source material in activated binder systems. This waste material is either being landfilled or used in limited amounts in fiberglass and paint manufacture. A Class F fly ash conforming to ASTM C 618 [25] is used in this study. The chemical composition of these starting materials are given in Table 1 and their particle size distributions, obtained using a laser particle size analyzer are shown in Fig. 1. Both glass powder and fly ash have very similar particle size distributions. The ground granulated blast furnace slag used in the ternary blends is a Type 100 slag conforming to ASTM C 989 [26], and the metakaolin for the ternary blends is classified as a Class N pozzolan according to ASTM C 618 [25]. Slag and metakaolin were used as materials to partially replace glass powder in order to improve the stability of these binders under exposure to moisture. The slag used has a median particle size ($d_{50}$) of 8 μm and metakaolin has a $d_{50}$ of 4 μm. The chemical compositions of these materials also can be found in Table 1. Laboratory grade NaOH beads were dissolved in water to produce the activator solutions of desired concentration (4, 6, or 8 M). The solutions were prepared and allowed to return to ambient temperature before used in the mixtures in order to negate the effect of high temperatures caused by the dissolution of NaOH in water. Mortars were prepared with glass powder alone, 50% glass powder-50% fly ash (by mass) or fly ash alone as the starting materials. River sand ($d_{50}$ of 0.6 mm) was used as the filler in mortars, which were proportioned using a liquid-to-powder ratio of 0.50, with approximately 40% paste volume fraction. The binder pastes used for the microstructural studies had a liquid-to-powder ratio of 0.40 because the flowability of pastes with a liquid-to-powder ratio of 0.50 was very high.

The source materials were mixed together in dry form in a laboratory mortar mixer for 2 min. The activator solution was then gradually added to the dry material and mixed together until a uniform mixture was obtained. After mixing, the specimens were cast in 50 mm cube molds and vibrated on a table vibrator until a homogeneous mixture was achieved. The specimens were covered with plastic sheets and allowed to set for 24 h in ambient conditions before being removed from the molds, and then were placed in the curing oven at the desired curing temperatures for the chosen durations. Heat curing was carried out at 50 °C and 75 °C for 24, 48, or 72 h.

**Table 1**
Chemical composition and properties of the starting materials.

| Composition (% by mass) | Glass powder | Fly ash | Metakaolin | Slag |
|---|---|---|---|---|
| $SiO_2$ | 72.5 | 50.2 | 48.9 | 36.0 |
| $Al_2O_3$ | 0.40 | 28.8 | 44.6 | 10.5 |
| $Fe_2O_3$ | 0.20 | 5.72 | 0.47 | 0.67 |
| CaO | 9.70 | 5.86 | – | 39.8 |
| MgO | 3.30 | 1.74 | – | 7.93 |
| $Na_2O$ | 13.7 | 0.96 | – | 0.27 |
| $K_2O$ | 0.10 | – | 0.24 | 0.16 |
| $TiO_2$ | – | – | 1.44 | – |
| $SO_3$ | – | 0.51 | – | 2.11 |
| LOI | – | 2.80 | – | 3.0 |
| Fineness, % passing 45 μm sieve | 74 | 75 | 100 | 95 |

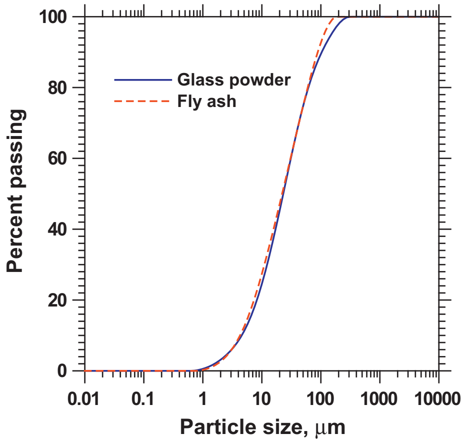

**Fig. 1.** Particle size distributions of glass powder and fly ash.

The compressive strengths of the mortar cubes were tested after the respective curing regime (thermal curing, or moist curing after heat curing to determine hydrolytic stability) and after they returned to ambient conditions. To understand the morphology and the composition of the reaction products formed in NaOH activated glass powder pastes, morphological analysis was performed on Au sputter-coated samples using Scanning Electron Microscopy (SEM) coupled with Energy dispersive X-ray analysis (EDX). The samples for Fourier Transform Infrared (FTIR) spectroscopy were prepared by mixing approximately 1 mg of sample with 300 mg of KBr. The spectra of the reaction products at desired ages of curing were obtained using an ATI Mattson FTIR spectroscope in the wavenumber range of 4000–400 $cm^{-1}$ at a resolution of 1 $cm^{-1}$.

## 3. Results, analysis, and discussion

### 3.1. Compressive strengths of NaOH activated glass powder mortars

The compressive strengths of mortars made using glass powder or fly ash alone or a combination of 50% of each of these materials by mass as the source materials are reported and discussed in this section. Two different NaOH concentrations, 4 M and 8 M, and two different curing temperatures, 50 °C and 75 °C were adopted for this part of the study. Since the specimens cured for 24 h at 50 °C did not develop considerable strength, the curing durations adopted at this temperature were 48 and 72 h. Similarly, when the curing temperature was 75 °C, a duration of 72 h resulted in significant specimen cracking especially for the glass powder mortars, and therefore the curing durations at this temperature were restricted to 24 and 48 h.

Fig. 2(a) and (b) depict the changes in the compressive strengths of NaOH activated mortars as a function of the glass powder content for different NaOH concentrations, curing temperatures, and curing durations. It is noted that, in general, addition of glass powder increases the compressive strength of the activated mortars. The only exception is for the 8 M NaOH activated mixtures subjected to 75 °C for 48 h, where the 50% fly ash–glass

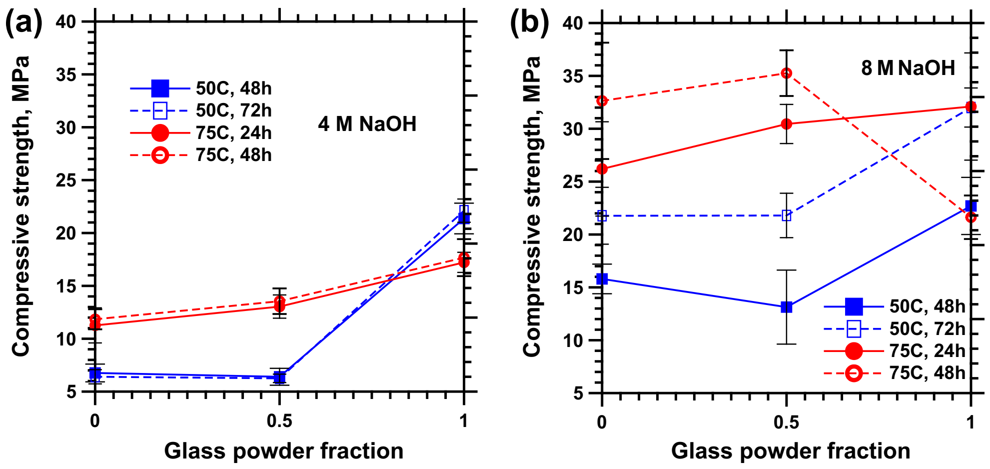

**Fig. 2.** Influence of glass powder content on the compressive strengths of NaOH activated mortars cured at 50 °C or 75 °C for 24, 48, or 72 h for activator concentrations of: (a) 4 M, and (b) 8 M.

powder blend shows the highest compressive strength. There is a significant increase in compressive strength when the alkali concentration is increased, indicating that higher alkali concentrations result in the formation of increased amounts of reaction products (sodium aluminosilicate (N–A–S–H) gel) from fly ash activation [7,27].

When glass powder is activated with NaOH, compressive strength increases when the NaOH concentration is increased from 4 M to 8 M, although the effect is not as dominant as that for mixtures containing fly ash. This suggests that increasing the activator concentration beyond a certain level might not be very critical for glass powder activation. This is attributed to the fact that there is very little alumina in glass powder to form N–A–S–H gel, and thus the reaction product formed is primarily a sodium silicate gel. This is confirmed later using electron micrographs as well as EDX and FTIR spectroscopic analyses. With increasing concentration of NaOH and the availability of reactive silica from glass powder, additional sodium silicate gel is formed that is hardened by the provision of external heat, resulting in some amount of strength enhancement. However, the gel formed in this case has a lower $SiO_2$-to-$Na_2O$ ratio (silica modulus) that has inferior mechanical properties than the gel with a higher modulus [28]. Sodium silicate gels also demonstrate higher amounts of shrinkage and cracking [29], which is shown in the micrographs in a later section.

It is noticed from Fig. 2(a) and (b) that a higher temperature always results in better compressive strengths for the activated binders containing fly ash (both 100% fly ash and 50% glass powder–fly ash blends) irrespective of the curing duration. On the contrary, for the glass powder mortars, the highest compressive strengths are obtained when the specimens are heat cured for a longer duration at a lower temperature or for a shorter duration at a higher temperature. It is well known that heating and loss of water facilitates the polymerization reaction and consequently gel hardening. It is conceivable that the physically bound water on the silanol groups on the surface of the sodium silicate gel, which accounts for a significant proportion of water contained in sodium silicate gels, could have been partly removed when the combination of curing temperature and duration is higher, resulting in gel shrinkage and cracking and consequently lower strengths under such conditions. Microscopic (Section 3.2) and spectroscopic (Section 3.3.2) evidence of this are presented in forthcoming sections.

For the mortars activated using 4 M NaOH, an increase in curing duration from 48 to 72 h at a temperature of 50 °C or from 24 to 48 h at 75 °C result in little to no strength enhancement, indicating that at lower alkali concentrations, the heat curing duration is not a significant parameter at the temperatures considered. For the 8 M NaOH activated mortars, increasing the curing duration from 48 to 72 h at a temperature of 50 °C results in appreciable strength gain, attributable to the combined effects of the higher alkalinity that results in faster reaction product formation, and the longer heat curing duration that ensures further progress of diffusion controlled reaction especially in activated mortars containing fly ash. When the heat curing duration is increased from 24 to 48 h at a temperature of 75 °C, a strength loss is observed for the 100% glass powder mortar. This can plausibly be ascribed to gel cracking and deterioration when sodium silicate gel is a reaction product.

### *3.2. Microscopic analysis of NaOH activated glass powder systems*

Electron micrograph of an unreacted glass powder particle is shown in Fig. 3(a), to demonstrate its surface characteristics and smooth, unfractured nature of the particle. Fig. 3(b) shows the microstructure of 4 M NaOH activated glass powder pastes heat cured at 75 °C for 48 h, and Fig. 3(c) shows the EDX spectra of a representative location (Point 1) in the microstructure. The silica in the glass powder has reacted with the alkalis forming sodium silicate gel. The EDX spectrum shows dominant peaks of Na and Si only. Micro-cracks are observed in the gel, which is believed to be a result of heat curing induced gel shrinkage. In a later section, Environmental SEM (ESEM, which avoids issues with dehydration under vacuum) micrographs are presented which also show the presence of cracks. The microstructure of 8 M NaOH activated glass powder paste, cured at 75 °C for 24 h is shown in Fig. 3(d). The reaction product is still continuous, and the corresponding EDX spectra detected the presence of Na and Si only in the reaction product. Analysis of EDX spectra of 5–7 points (believed to be adequate because of the homogeneity of the gel) on both these microstructures showed that the average Si/Na atom ratio of the gel is lowered for the mixture activated using a higher concentration of the activator (from 3.62 for the gel in Fig. 3(b) to 2.65 for the gel in Fig. 3(d)), which is along expected lines. The higher amounts of network modifiers such as sodium (which reduces the gel modulus) increases the number of non-bridging oxygen (NBO) sites [26]. This changes the connectivity of the $SiO_4$ tetrahedral network [30], resulting in structural changes in the amorphous sodium silicate phase. A quantification of the structural changes can only be demonstrated through characterization techniques such as $^{29}$Si

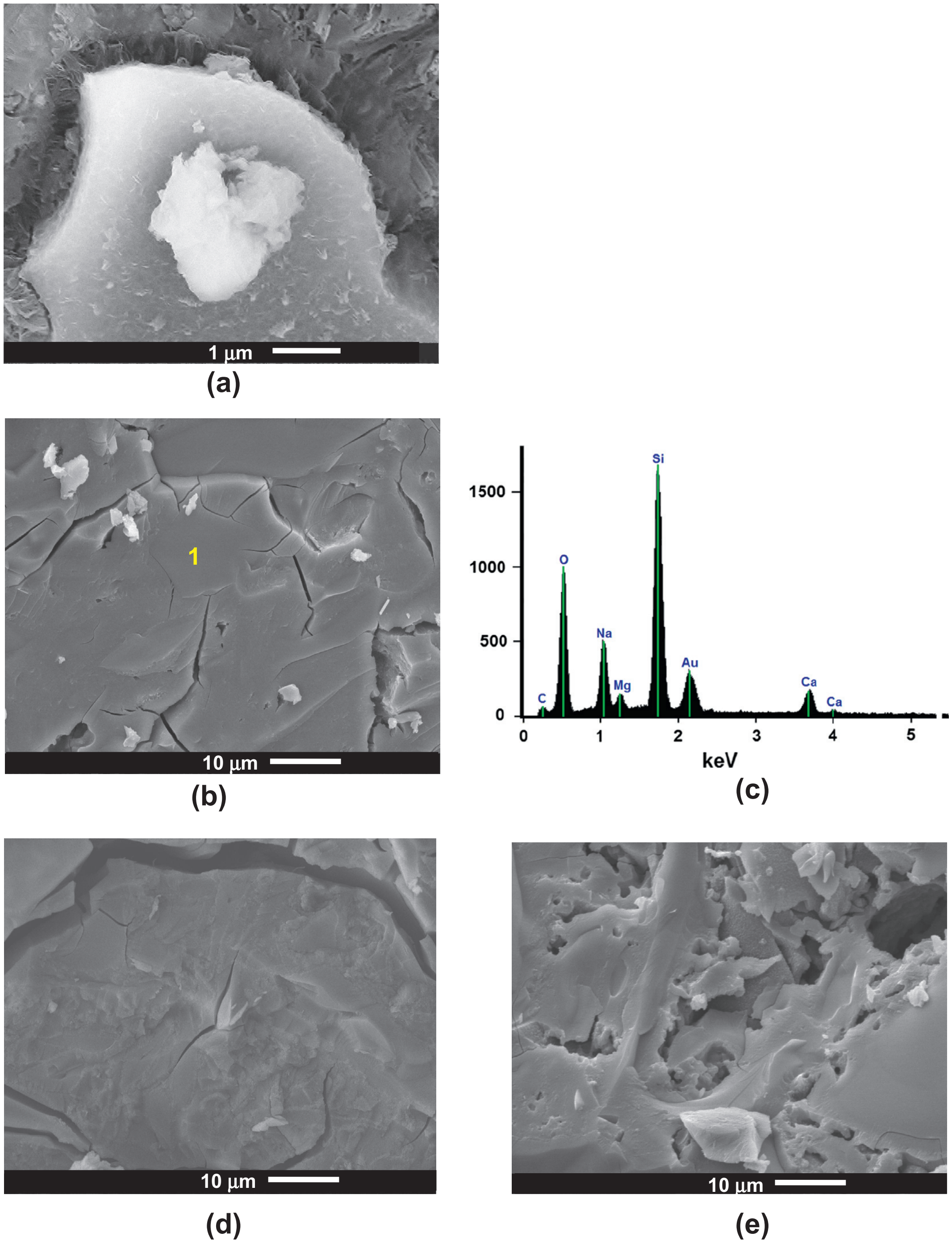

**Fig. 3.** (a) Scanning electron micrograph of an unreacted glass powder, (b) and (c): SEM and EDX spectra corresponding to Point 1 in (a) for 100% glass powder paste activated using 4 M NaOH and heat cured for 48 h at 75 °C, (d) SEM of 100% glass powder paste activated using 8 M NaOH and heat cured for 24 h at 75 °C, (e) same mixture as in (d), but heat cured for 48 h at 75 °C.

NMR. Another additional level of complexity arises from the uncertainties in the distribution of the network modifiers (whether they are clustered into areas rich in NBO and rich in Si, or distributed randomly) in the gel structure [31]. These aspects are beyond the scope of the present study.

When the microstructure of 8 M NaOH activated glass powder pastes cured at 75 °C for an even longer duration of 48 h is considered, a very different picture emerges as shown in Fig. 3(e). The microstructure is very porous, and the gel can no longer be described as continuous. Heat curing for longer durations and the presence of higher alkalinity in the pore solution induces disintegration of the gel, resulting in the microstructure shown in Fig. 3(e). The compressive strength of this mixture is lower than that of the one cured for only 24 h. The discussions above throw light into the combined effects of alkalinity and the heat curing duration on the microstructure and consequently the properties of NaOH activated glass powder binders.

The microstructure of a 50% glass powder–fly ash blend, activated by 8 M NaOH and heat cured at 75 °C for 48 h is shown in Fig. 4. The reaction product is found to be a mixture of N–A–S–H

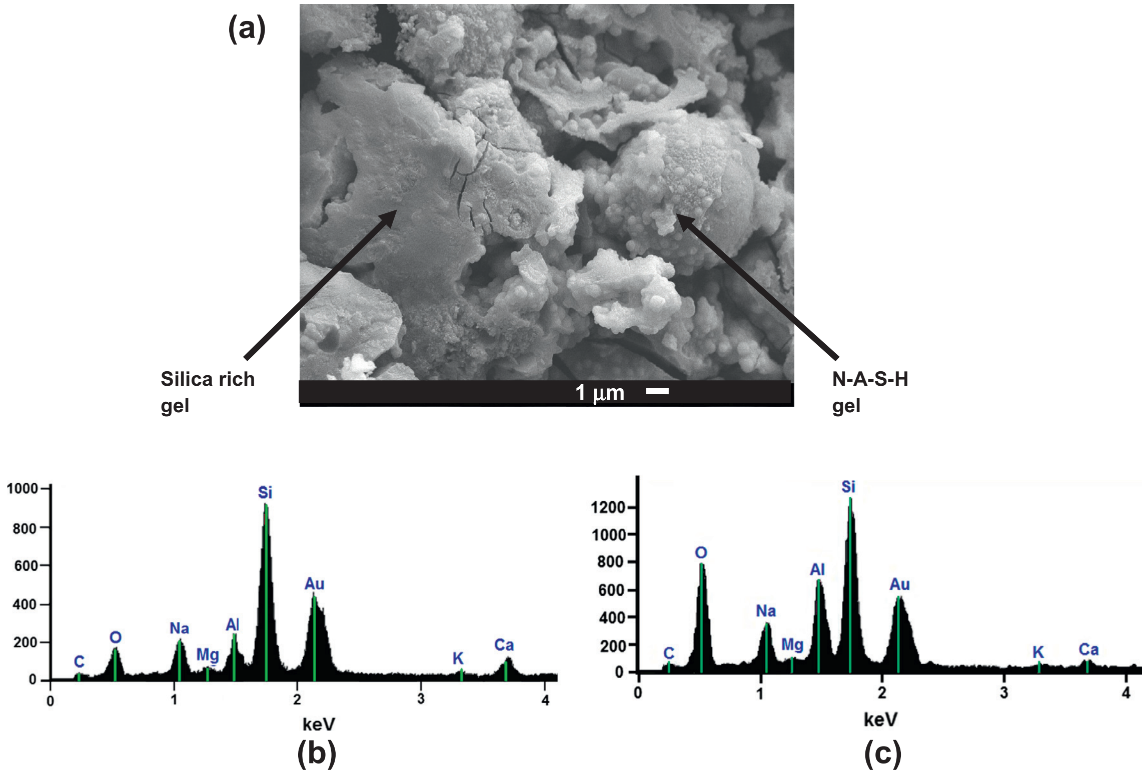

**Fig. 4.** (a) Micrograph of a 50% glass powder – fly ash blend activated using 8 M NaOH and heat cured for 48 h at 75 °C, (b) EDX spectra of the smooth silicate gel, and (c) EDX spectra of N–A–S–H gel.

and sodium silicate gels. The N–A–S–H gel is formed around the fly ash particles [4,7,13,27], whereas the locations previously occupied by the glass powder are transformed into a sodium silicate gel. The EDX spectra shown in Fig. 4 confirm this observation, even though the sodium silicate gel contains traces of Al. Some dissolved Al from fly ash might have diffused into areas near the glass powder particles. Silicate gels are reported to have a high affinity for Al. Al can be incorporated into the silica tetrahedron with Na in a charge balancing role and/or adsorbed in the gel surface with Al retaining an octahedral configuration [32]. The mechanism of Al incorporation also dictates its amount in the gel. The Si/Na and Si/Al atom ratios for the sodium silicate gel are found to be higher than the corresponding values for the N–A–S–H gel.

### 3.3. *Stability of the reaction products under exposure to moisture*

The moisture stability of conventional cement hydration products such as C–S–H gel and alkali activated aluminosilicate reaction products such as N–A–S–H are well documented. With regards to sodium silicate, the moisture stability is a function of the silica modulus of the produced gel [28,33]. This, in turn, is dependent on the source material and activator chemistry as well as the processing conditions.

#### 3.3.1. *Compressive strength loss as an indicator of moisture instability*

Fig. 5(a) and (b) depict the compressive strength changes in 4 M and 8 M NaOH activated mortars respectively as a function of the exposure duration to moisture (cured in a fog spray chamber) after heat curing at 75 °C for 24 h. The fly ash mortars show no strength loss, but in both the cases, the activated glass powder mortars show the highest strength loss after 28 days of curing in a moist environment, followed by the glass powder–fly ash blended mortar. For the mortars containing glass powder, the most significant strength loss under this exposure regime is observed for the first 7 days and then the strength loss is gradual. When the sodium silicate gels are exposed to water, sodium will be leached out as shown below:

$$\equiv\text{Si—O—Na} + \text{H}_2\text{O} \rightarrow \equiv\text{Si—O—H} + \text{Na}^+ + \text{OH}^-. \quad (1)$$

Further dissociation depends on the continuing hydrolysis of $\equiv$Si–O–Si$\equiv$ linkages. When the specimens are subjected to moist environment in a fog sprayed curing room (>98% RH) as was the case for the results shown in Fig. 5, the pH of the environment does not change significantly with exposure duration, even though a slight localized increase in pH can be expected around the specimen due to the leaching of $\text{OH}^-$ ions. The surface of the gel becomes alkali depleted and a silica rich layer might form on the surface. This will limit further silica dissolution, resulting in a reduced degree of strength loss after the initial dissociation period, as observed in Fig. 5.

If the specimens are immersed in an aqueous environment, the pH of the solution increases because of the alkalinity produced by the reaction shown in Eq. (1). The alkaline environment attacks the Si–O–Si bonds to further dissociate the silica [34] as shown in following equation:

$$\equiv\text{Si—O—Si}\equiv + \text{OH}^- \rightarrow \equiv\text{Si—OH} + \equiv\text{Si—O}^- \quad (2a)$$

$$\equiv\text{Si—OH} + \text{OH}^- \leftrightarrow \equiv\text{Si—O}^- + \text{H}_2\text{O}. \quad (2b)$$

To investigate the silica gel dissolution in such an environment, 8 M NaOH activated glass powder, and 50% glass powder–fly ash blends were stored in 0.5 M NaOH solution (pH of 13.7) after heat curing at 75 °C for 24 h. An alkaline storage medium is used because Eqs. (2a) and (2b) are catalyzed by hydroxyl ions, and the reactions go to completion only in solutions with sufficient alkalinity [35]. The dependence of the rate and extent of dissolution of the

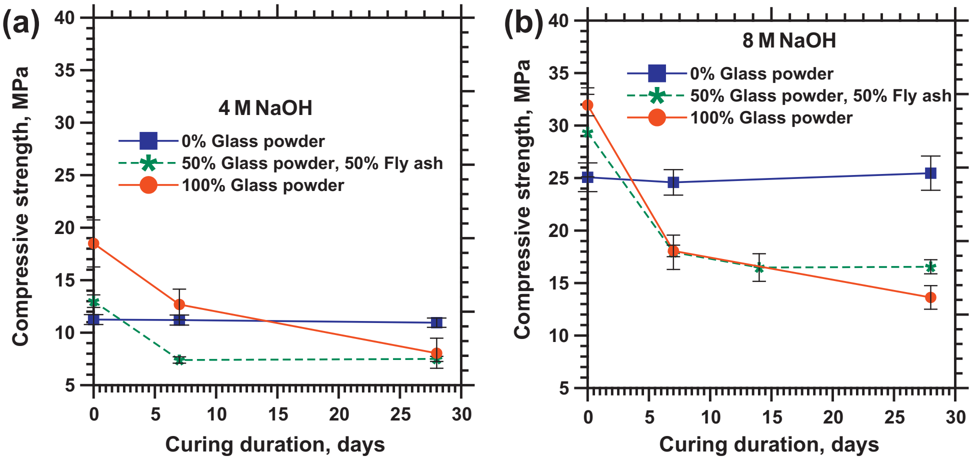

**Fig. 5.** Compressive strength as a function of moist curing duration for the glass powder, fly ash, and blend mortars activated using: (a) 4 M NaOH, (b) 8 M NaOH.

silicate gel on the alkali metal cation type and the attainment of equilibrium between the different oligomeric types have been explained in [33]. A comparison of strength loss on exposure to moisture under both the conditions is shown in Fig. 6. It can be noticed that the strength loss is higher when the specimens are immersed in an alkaline solution, because of the reasons stated above. Even if it is considered that the leaching process facilitates additional reaction product formation because of the exposure of the hitherto unreacted starting materials to the highly alkaline pore solution, the strength loss because of the gel instability is found to be higher than the strength enhancement thus achieved. The masses of the saturated specimens (100% glass powder activated using 8 M NaOH and cured at 75 °C for 24 h) before the start of the exposure in the alkaline media and after 7 days of exposure indicated a porosity enhancement in excess of 20%.

The 50% glass powder–fly ash blend shows a residual strength of about 56% when exposed to moisture in a fog-spray chamber, while it drops to 35% when immersed in an aqueous solution. For the 100% glass powder mortars, the strength loss is more drastic – a residual strength of 42% when exposed to moisture in the fog-spray chamber, and only 24% when immersed in an aqueous solution. After about 14 days of exposure to either of the conditions, the glass power–fly ash blend does not lose any further strength. For the 100% glass powder blend, strength loss occurs throughout the entire exposure duration, demonstrating the lack of continued moisture stability of the reaction products.

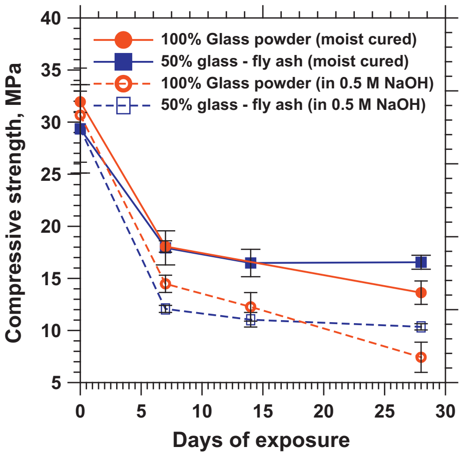

**Fig. 6.** Compressive strength of the glass powder mortars as a function of exposure duration, when exposed to moisture in a fog-spray chamber or immersed in a 0.5 M NaOH solution after heat curing at 75 °C for 24 h.

### *3.3.2. Microstructural and spectroscopic analysis of hydrolytic instability*

Fig. 7(a) and (b) show the microstructures of 8 M NaOH activated glass powder paste cured at 75 °C for 24 h, before and after 3 days of immersion in deionized water. It appears that portions of the reaction product are breaking away from the paste that is exposed to moisture. This is responsible for some of the strength loss at early periods of moisture exposure as shown in Fig. 6. Fig. 7(c) and (d) depict the ESEM micrographs of the same specimen (8 M NaOH activated glass powder paste, cured at 75 °C for 24 h) before and after exposure to 10 days of immersion in water. A significantly higher degree of paste deterioration can be observed in Fig. 7(d), where the homogeneous structure of the pre-exposure reaction product is non-existent. The influence of immersing the specimen in an aqueous environment and the duration of exposure on the property loss, as quantified from the strength results in Fig. 6 are visually confirmed through these micrographs. Fig. 7(e) and (f) show the pre- and post-exposure ESEM micrographs of the 50% glass powder–fly ash blend paste. The exposure condition was similar to that of the specimen shown in Fig. 7(d). The exposure has resulted in loss of reaction products, as was confirmed from the strength loss.

Fig. 8 presents the FTIR spectra of the 8 M NaOH activated glass powder, glass powder–fly ash blend, and the fly ash binders before and after 10 days of immersion in water. The major bands observed in these spectra, other than the stretching and deformation modes of $OH^-$ observed at around 3400 $cm^{-1}$, are the ones associated with the Si–O–Si asymmetric stretching vibrations in the range of 1000–1050 $cm^{-1}$. For conventional C-S-H gel from cement pastes, the Si–O–Si stretching bands generally appear in the wavenumber range of 950–1000 $cm^{-1}$ [36], which is typical of a silica network that is not highly polymerized. Increase in silica polymerization shifts the Si–O–Si stretching vibration peaks to higher wavenumbers. The spectra (a) in Fig. 8 are for the 100% glass powder binder, before and after moisture exposure. The only reaction product for this binder is sodium silicate gel, where the peak of the Si–O–Si stretching vibration appears at a wavenumber of 1054 $cm^{-1}$ before moisture exposure. This is attributed to the presence of a polymerized silica rich gel in its microstructure. Pure silica shows a characteristic Si–O–Si stretching band at 1100 $cm^{-1}$ and the presence of network modifiers such as Na reduces the frequency. The predominance of $Q^2$ and $Q^3$ silicates in the gelatinous silicate phases results in wavenumbers in the 1000–1050 $cm^{-1}$

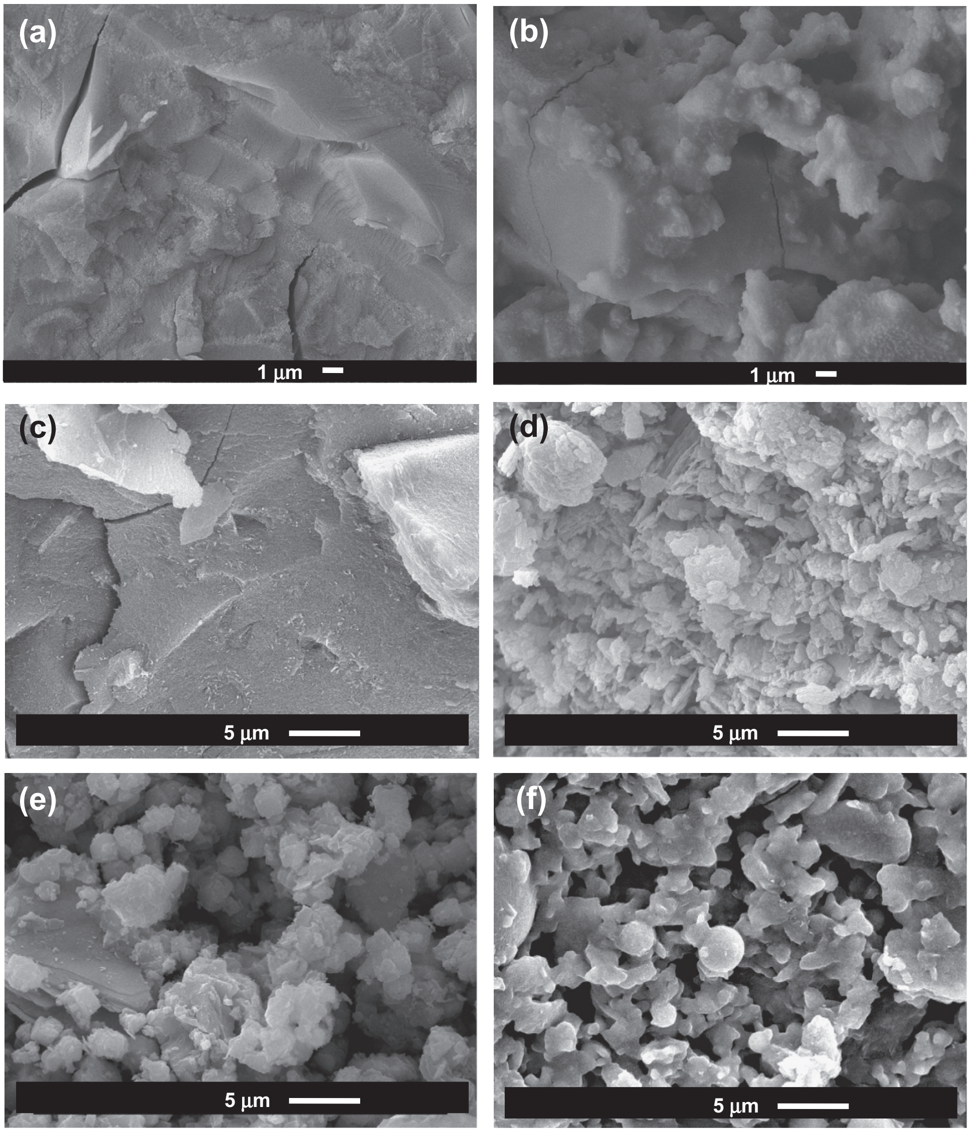

**Fig. 7.** (a) SEM image of 8 M NaOH activated glass powder paste heat cured for 24 h at 75 °C; (b) exposed to moisture in a fog chamber for 3 days after the curing regime of (a); (c) ESEM image of the specimen shown in figure (a); (d) ESEM image of the specimen in (c) immersed in water for 10 days; (e) ESEM image of 8 M NaOH activated 50% glass powder–fly ash blend heat cured for 24 h at 75 °C; (f) ESEM image of the specimen in (e) immersed in water for 10 days.

range, where as a predominance of $Q^1$ and $Q^2$ silicates results in wavenumbers in the 950–1000 $cm^{-1}$ range as is typically observed for conventional C–S–H. After the moisture exposure, the peak of the Si–O–Si stretching vibration shifts to a wavenumber of 1019 $cm^{-1}$ (from 1054 $cm^{-1}$) for the activated glass powder pastes. This can be construed as an indication of the depolymerization of silica network [37], as conjectured from the results on compressive strength loss and observed from the micrographs in Fig. 7. Note that the peak locations in the FTIR spectra could be the composite signatures that account for the Si–O–Si vibrations in the other components present in the reaction products as well. However their relative shifts provide a qualitative indication of the moisture induced disintegration of the reaction products that manifest in the mechanical property reduction. For the NaOH activated fly ash paste, there is no change in the location of the Si–O–Si stretching peak before and after moisture exposure as shown in spectra (b) of Fig. 7, attesting to the moisture stability of the N–A–S–H gel produced.

When the FTIR spectra for the 50% glass powder–50% fly ash binder as shown in spectra (c) of Fig. 8 are observed, it can be seen that the wavenumber corresponding to Si–O–Si stretching vibration changes from 1026 $cm^{-1}$ before the exposure to 1017 $cm^{-1}$ after the exposure, i.e., the severity of depolymerization as observed from FTIR spectra is apparently reduced, owing to the presence of fly ash that results in the formation of N–A–S–H gel, and the consequent changes in the sodium silicate gel (with respect to its $SiO_2$-to-$Na_2O$ ratio, and potential incorporation of Al as shown in an earlier section) that makes it more resistant to depolymerization. The characteristic wavenumber for the non-exposed reaction product lies between that of the sodium silicate gel from glass powder reaction (~1054 $cm^{-1}$) and that of N–A–S–H gel from fly ash activation (~1016 $cm^{-1}$).

In Section 3.1, it was mentioned that the physically bound water from the silanol groups on the surface of the sodium silicate gel could have been removed as a result of heat curing for longer times or at higher temperatures. The physically bound water in silanol groups show characteristic IR bands in the 3400–3460 $cm^{-1}$ range (difficult to detect because of the interference with the other $OH^-$ groups) and around 1630 $cm^{-1}$ [28]. From the FTIR spectra shown in Fig. 8(a) and (c) for the pastes containing glass powder (where sodium silicate gel is formed as a reaction product), peaks at around 1630 $cm^{-1}$ are absent before the exposure to moisture,

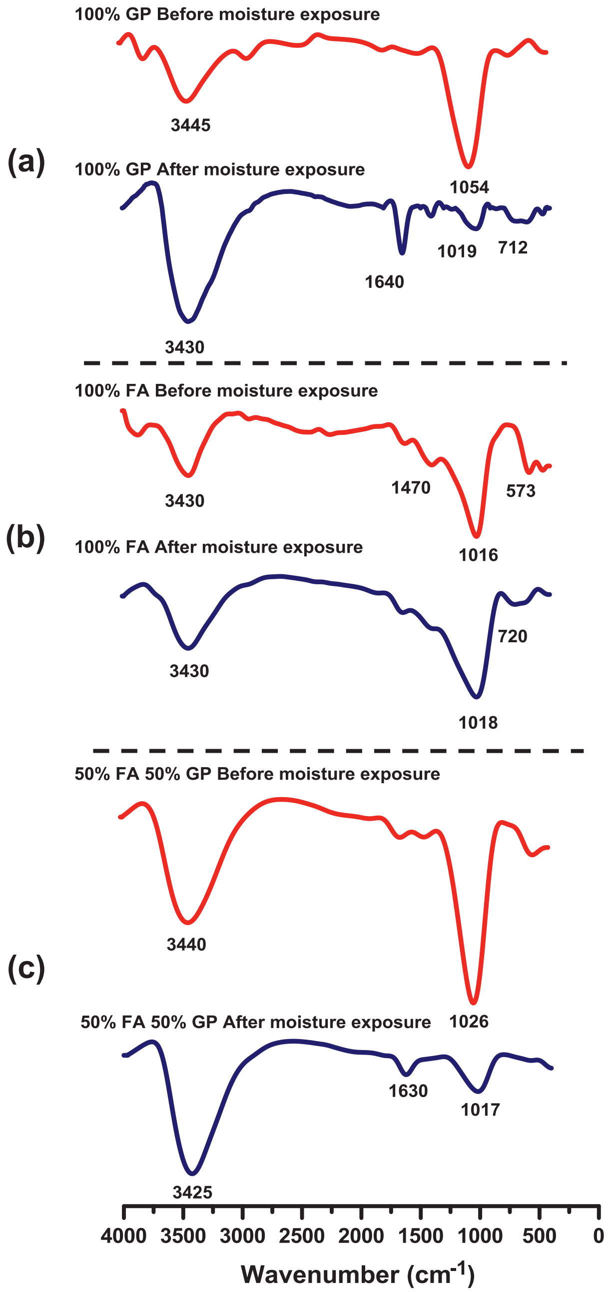

**Fig. 8.** FTIR spectra before and after exposure to moisture of: (a) 100% glass powder paste, (b) 100% fly ash paste, and (c) 50% glass powder – 50% fly ash paste. All the pastes were activated using 8 M NaOH and heat cured for 24 h at 75 °C.

i.e., after the heat curing duration. However, when these specimens were subjected to moisture again, distinct bands at 1630–1640 $cm^{-1}$ make their appearance, suggesting that heat curing removes the physically bound water from the silanol groups on the surface of the sodium silicate gel.

### 3.4. Methods to mitigate strength loss on exposure to moisture

The foregoing discussions clearly demonstrate the lack of moisture stability in sodium silicate gels obtained as reaction products when mixtures containing glass powder are activated using NaOH. The behavior was not very different when sodium silicate powder of different $SiO_2$-to-$Na_2O$ ratios was used as the activating agent [38]. Hence, this section explores means to obtain stable reaction products in activated glass powder binder systems by changing the source material constitution. The glass powder is retained as the major source material (50% by total mass of the binder).

#### 3.4.1. Addition of Al and Ca containing source materials

One of the straightforward means of accomplishing reaction product stability is to ensure the formation of a sodium aluminosilicate (N–A–S–H) gel through doping the system with external reactive alumina. Higher cross-linking offered by the presence of Al is expected to reduce the solubility and lead to a stable microstructure. The replacement of $Si^{4+}$ with $Al^{3+}$ immobilizes an alkali ion that is needed for charge balance, thus limiting the dissociation. As seen thus far in this study, replacing 50% of the glass powder by Class F fly ash does not seem to be sufficient to produce a moisture resistant reaction product. A reduction in the Si/Al ratio of the sodium silicate gel that is required to ensure moisture stability [39] is likely to be achieved by a further increase in the fly ash proportion in the mixture (this also depends on how much Al diffuses into the sodium silicate gel structure and gets incorporated in it, as explained in Section 3.2), but such an attempt is not made because the intention of this study is to facilitate the preparation of moisture resistant reaction products from glass powder as the major source material. Hence metakaolin which contains more reactive alumina than fly ash was used in this phase of the work. However, a replacement of up to 25% of the fly ash from the blended mixture to produce 50% glass powder–25% fly ash–25% metakaolin systems did not result in a reaction product that was moisture stable as observed from compressive strength results before and after exposure to moisture. Additions beyond 25% by mass of metakaolin were impractical because of the high water demand of metakaolin that created issues with proper mixing and placing.

Another option considered was to incorporate Ca into the reaction products. The incorporation of each atom of Ca into the silicate gel structure produces two NBOs; however the alkaline earth ions are less mobile than the alkali ions and therefore can be expected to block alkali diffusion [34]. Other possible means through which the Ca incorporation in the silicate gel structure facilitates reduces dissociation are: (i) the divalent Ca ion acts as a structural link between the neighboring NBOs and thus maintains the network connectivity as opposed to the Na ion that only balances the charge on the neighboring NBO, and (ii) the $Ca^{2+}$ ion has a much greater electrical field strength than the $Na^{+}$ ion, allowing it to have a larger effect on the strength of the bonds in the silicate network [40], thereby reducing dissociation. In addition, Ca addition opens up the possibility of formation of C–(A)–S–H gel as a reaction product. Therefore, ternary blends containing 50% glass powder by mass, and the remaining 50% made up of a combination of ground granulated blast furnace slag as the Ca source and metakaolin as the Al source were proportioned. It has been reported that binary blends of slag and metakaolin compete for Si species since both Ca and Al require Si to form reaction products [41]. Since there is an abundance of silica in the glass powder, Ca and Al silicates can form as the reaction products.

#### 3.4.2. Strength, microstructure, and hydrolytic stability of ternary blends

Fig. 9(a)–(c) show the compressive strength variation of mortars activated using varying concentrations of NaOH as a function of moist curing duration after heat curing at 75 °C for 24 h. The binders, the results for which are shown in these graphs, consist of: (i) 100% glass powder, (ii) 50% glass powder, 25% slag, and 25% metakaolin, and (iii) 50% glass powder, 35% slag, and 15% metakaolin. When compared to the plain glass powder system, both the examined ternary blends were able to better control the strength loss occurring as a result of exposure to moisture. The ternary blend containing a higher amount of slag is found to have the

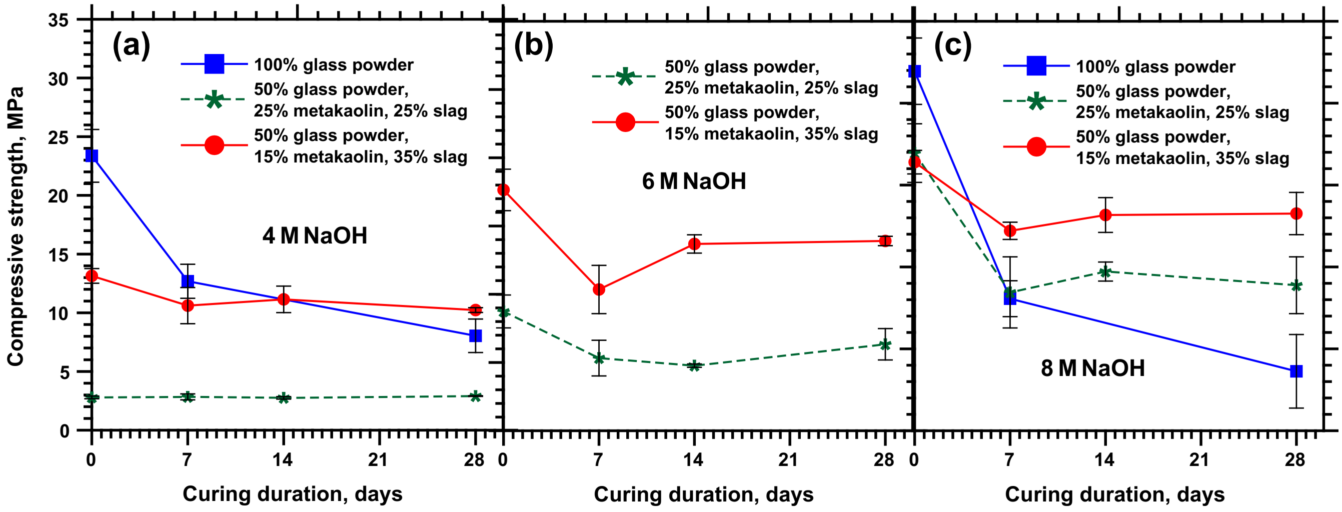

**Fig. 9.** Compressive strength of ternary blend mortars (glass powder – metakaolin – slag) as a function of moist curing duration for mortars activated using: (a) 4 M NaOH, (b) 6 M NaOH, and (c) 8 M NaOH.

highest strength at the end of the moist curing duration. For example, the ternary blend with 35% slag and 15% metakaolin activated using 8 M NaOH retains 90% of its heat cured strength after 28 days of moist curing whereas the 25% slag–25% metakaolin blend retains 70% of its heat cured strength. This is a significant improvement over the 100% glass powder mixture which retained only 42% of its heat cured strength or the 50% glass powder–50% fly ash blend that retained only 55% of its heat cured strength.

It is observed from these figures that the highest strength before moist curing is invariably obtained for the 100% glass powder mixtures. For the 4 M NaOH activated blends, the mixture containing a higher amount of metakaolin shows lower strength after heat curing, whereas for the 8 M NaOH activated blend, the strength of this mixture is much higher indicating that a higher alkalinity is necessary to accelerate the geopolymerization process. Ca based reaction products can be expected to form along with N–A–S–H and sodium silicate gels in these ternary binders. Detailed mechanisms for the metastable co-existence of the Ca based reaction products and the alkali aluminosilicate gel has been presented in [42].

Both the ternary blends show an initial strength loss when exposed to moisture after the heat curing duration. This could be attributed to: (i) the presence of some amount of dissolution-prone sodium silicate gel formed from the glass powder reaction, and (ii) the fact that the strength testing was conducted on a relatively dry specimen after heat curing and on a wet specimen after moisture exposure (apparent compressive strengths are higher when tested dry). The FTIR spectra for the 50% glass powder–35% slag–15% metakaolin ternary blend before and after 10 days of immersion in water, shown in Fig. 10, do not indicate noticeable shifts in the Si–O–Si stretching peak. It is possible that some silica dissolution could have occurred, but they preferentially reacted with dissolved Ca than polymerize with the soluble aluminates, forming calcium bearing reaction products, that facilitate a strength increase under further moisture exposure. A slight strength increase is observed for the blends with a higher amount of slag as seen in Fig. 9(a)–(c). The low Ca/Si molar ratio products thus formed also show higher wavenumbers for the Si–O–Si stretching band than those in the conventional C–S–H gel [43], thereby potentially masking the effects of sodium silicate gel depolymerization.

For the ternary blend with a higher metakaolin content activated by 8 M NaOH, there is a significant strength loss at early times of exposure to moisture. Higher activator alkalinity coupled with the higher alumina content and the larger surface area of metakaolin facilitates N–A–S–H gel formation, and the further uptake of Na to form the reaction products is slowed down (the reaction becomes diffusion controlled). It is suggested here that the sodium silicate gel that is formed does not have sufficient moisture stability because of its lower modulus [28] resulting from the higher activator alkalinity. The dissolution of this sodium silicate under moisture exposure results in the observed strength loss. On the other hand, for the activated blend with a higher slag content, the reaction product formed consists of C–(A)–S–H gel (from slag), some amount of N–A–S–H gel (from metakaolin), and potentially a high modulus sodium silicate gel (from glass powder). Here, the sodium silicate gel is rendered more moisture resistant by the partial replacement of $Na^+$ by $Ca^{2+}$ in the gel structure and Al incorporation, the consequences of which were elucidated earlier.

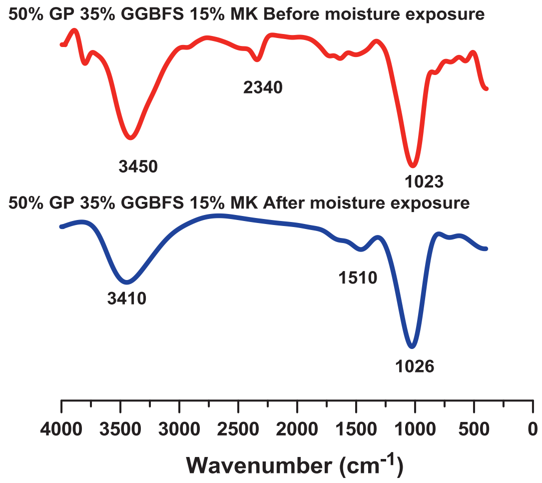

**Fig. 10.** FTIR spectra of the 50% glass powder – 35% slag – 15% metakaolin blend activated using 8 M NaOH and heat cured at 75 °C for 24 h, before and after exposure to moisture.

Microstructure (ESEM) of the high slag content ternary blend is shown in Fig. 11(a) and the EDX spectra of the indicated locations are shown in Fig. 11(b). The spectra indicate that N–A–S–H and Mg containing C–A–S–H gels are the reaction products in this case. The incorporation of Mg in the reaction products of alkali activated slag has been reported elsewhere [44]. The consumption of Na in a

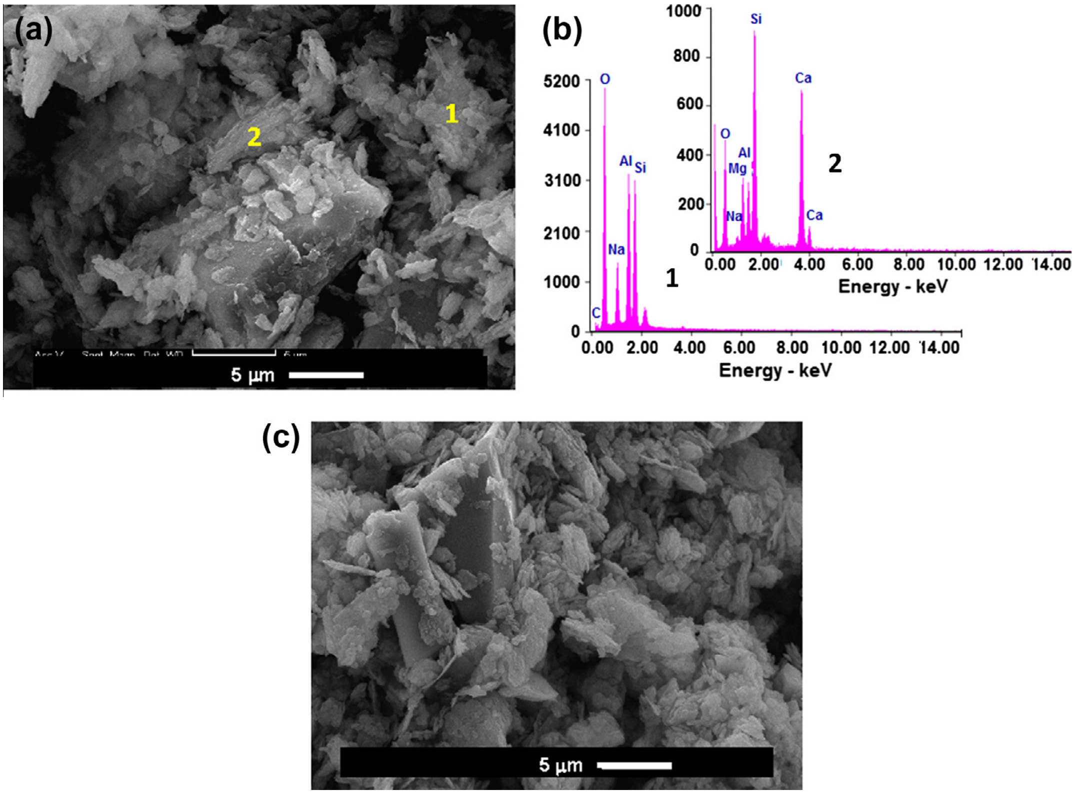

**Fig. 11.** (a) ESEM image of 8 M NaOH activated 50% glass powder – 35% slag – 15% metakaolin blend after heat curing at 75 °C for 24 h, (b) EDX spectra at the indicated locations showing N–A–S–H and C–A–S–H gels, (c) ESEM image of the specimen in (a) immersed in water for 10 days.

charge balancing role in N–A–S–H, the binding of some Na to C–S–H gel [45], and the incorporation of Ca and Al into the sodium silicate gel structure results in a reaction product that is more stable under moisture exposure than the ones formed either from the activation of pure glass powder or a 50% glass powder–fly ash blend. Fig. 11(c) shows the microstructure of this ternary blend after 10 days of immersion in water. The microstructure does not appear to be significantly altered by the exposure. The above discussions show that it is possible to further optimize the source material composition by carefully choosing the components so as to completely prevent the strength loss of these binders when exposed to moisture after heat curing.

## 4. Conclusions

This paper has discussed the strength development, microstructure and reaction products, and the hydrolytic stability of alkali activated binders where glass powder is used as the major source material. The major conclusions are listed below.

- Glass powder binders activated using higher concentrations of NaOH were found to have higher compressive strengths than the activated fly ash mixtures when heat cured at lower temperatures. Higher curing temperatures and durations adversely influenced the strength of glass powder binders when higher alkalinity was used in the activation process, demonstrated by a porous and disconnected microstructure.
- The lack of hydrolytic stability of sodium silicate gels formed in activated binders using glass powder alone was evident from the drastic strength loss under moist curing conditions. Silica depolymerization in sodium silicate gels of lower modulus could explain this strength loss.
- Retaining glass powder as a major constituent of the binders and doping the systems with Ca and Al through the use of ground granulated blast furnace slag and metakaolin respectively was found to better control the strength loss under moisture exposure. The reaction products in the ternary blended systems included C–A–S–H and N–A–S–H gels. It has been shown that, by carefully choosing the source materials so as to compositionally supplement the glass powder, alkali activated binders consisting of glass powder as the major component, with desirable mechanical and moisture-resistance characteristics could be produced.

## Acknowledgements

The glass powder was provided by Potters Industries, Potsdam NY, the slag by Holcim US, and the metakaolin by Burgess Pigments. The facilities of the Center for Advanced Materials Processing (CAMP) at Clarkson University and the Advanced Cementitious Materials and Systems Laboratory and LeRoy Eyring Center for Solid State Science at Arizona State University (ASU) are acknowledged.

## References

[1] Gartner E. Industrially interesting approaches to “low-$CO_2$” cements. Cem Concr Res 2004;34:1489–98.
[2] Duxson P, Provis JL, Lukey GC, van Deventer JSJ. The role of inorganic polymer technology in the development of ‘green concrete’. Cem Concr Res 2007;37:1590–7.
[3] Davidovits J. Geopolymers: inorganic polymeric new materials. J Therm Anal 1991;37:1633–56.
[4] Palomo A, Grutzeck MW, Blanco MT. Alkali activated fly ashes – a cement for the future. Cem Concr Res 1999;29:1323–9.

[5] Shi C, Krivenko PV, Roy D. Alkali-activated cement and concretes. New York: Taylor and Francis; 2006.
[6] Provis JL, Yong CZ, Duxson P, van Deventer JSJ. Correlating mechanical and thermal properties of sodium silicate-fly ash geopolymers. Colloid Surfaces A: Physicochem Eng Aspects 2009;336:57–63.
[7] Bakharev T. Geopolymeric materials prepared using Class F fly ash and elevated temperature curing. Cem Concr Res 2005;35:1224–32.
[8] Wang SD, Scrivener KL. Hydration products of alkali activated slag cement. Cem Concr Res 1995;25:561–71.
[9] Puertas F, Martínez-Ramírez S, Alonso S, Vázquez T. Alkali activated fly ash/slag cement – strength behavior and hydration products. Cem Concr Res 2000;30:1625–32.
[10] Xie Z, Xi Y. Hardening mechanisms of an alkaline-activated Class F fly ash. Cem Concr Res 2001;31:1245–9.
[11] Fernández-Jiménez A, Palomo JG, Puertas F. Alkali activated slag mortars – mechanical strength behavior. Cem Concr Res 1999;29:1313–21.
[12] Sakulich AR, Miller S, Barsoum MW. Chemical and microstructural characterization of 20 month old alkali activated slag cements. J Am Ceram Soc 2010;95:1741–8.
[13] Fernández-Jiménez A, Criado M. Microstructure development of alkali-activated fly ash cement: a descriptive model. Cem Concr Res 2005;35:1204–9.
[14] Kovalchuk G, Fernández-Jiménez A, Palomo A. Alkali-activated fly ash: effect of thermal curing conditions on mechanical and microstructural development – Part II. Fuel 2007;86:315–22.
[15] Duxson P, Provis JL, Lukey GC, Mallicoat SW, Kriven WM, van Deventer JSJ. Understanding the relationship between geopolymer composition, microstructure and mechanical properties. Colloids Surfaces A: Physiochem Eng Aspects 2005;269:47–58.
[16] Hajimohammadi A, Provis JL, van Deventer JSJ. The effect of silica availability on the mechanism of geopolymerization. Cem Concr Res 2011;41:210–6.
[17] Lloyd RR, Provis JL, van Deventer JSJ. Microscopy and microanalysis of inorganic polymer cements. 2: The gel binder. J Mater Sci 2009;44:620–31.
[18] http://www.epa.gov/osw/conserve/materials/glass.htm (last accessed 3.07.11).
[19] Schwarz N, Neithalath N. Influence of a fine glass powder on cement hydration: comparison to fly ash and modeling the degree of hydration. Cem Concr Res 2008;38:429–36.
[20] Shayan A, Xu A. Performance of glass powder as a pozzolanic material in concrete: a field trial on concrete slabs. Cem Concr Res 2006;36:457–68.
[21] Schwarz N, Cam H, Neithalath N. Influence of a fine glass powder on the durability characteristics of concrete and its comparison to fly ash. Cem Concr Compos 2008;30:486–96.
[22] Jain J, Neithalath N. Chloride transport in fly ash and glass powder modified concretes – influence of test methods on microstructure. Cem Concr Compos 2010;32:148–56.
[23] Torres JJ, Palacios M, Hellouin M, Puertas F. Alkaline chemical activation of urban waste glass to produce cementitious materials. In: Proceedings of the 1st Spanish national conference on advances in materials recycling and eco-energy, Madrid; 2009. p. 111–114.
[24] Bunker BC, Arnold GW, Beauchamp EK. Mechanisms of alkali leaching in mixed Na–K glasses. J Non-Cryst Solids 1983;58:295–322.
[25] ASTM C618-12a. Standard Specification for Coal Fly Ash and Raw or Calcined Natural Pozzolan for Use in Concrete. ASTM International, West Conshohocken, PA; 2012.
[26] ASTM C989-12a. Standard Specification for Slag Cement for Use in Concrete and Mortars. ASTM International, West Conshohocken, PA; 2012.
[27] Ravikumar D, Peethamparan S, Neithalath N. Structure and strength of NaOH activated concretes containing fly ash or GGBFS as the sole binder. Cement Concr Compos 2010;32:399–410.
[28] Dimas D, Giannopoulou I, Panias D. Polymerization in sodium silicate solution: a fundamental process in geopolymerization technology. J Mater Sci 2009;44:3719–30.
[29] Oyler DC. Use of a sodium silicate gel grout for plugging horizontal methane drainage holes. Bureau Mines Report Invest 1984;8843:25.
[30] Jones AR, Winter R, Greaves GN, Smith IH. MAS NMR study of soda-lime-silicate glasses with variable degree of polymerization. J Non-Cryst Solids 2001;293–295:87–92.
[31] Angeli F, Villain O, Schuller S, Ispas S, Charpentier T. Insight into sodium silicate glass structural organization by multinuclear NMR combined with first principles calculations. Geochim Cosmochim Acta 2011;75:2453–69.
[32] Stone WEE, El Shafei GMS, Sanz J, Selim SA. Association of soluble aluminum ionic species with a silica-gel surface. J Phys Chem 1993;97:10127–32.
[33] Wijnen PWJG, Beelen TPM, de Haan JW, Rummens CPJ, van de Ven LJM, van Santen RA. Silica gel dissolution in aqueous alkali metal hydroxides studied by $^{29}$Si-NMR. J Non-Cryst Solids 1989;109:85–94.
[34] Jantzen CM, Plodinec MJ. Thermodynamic model of natural, medieval, and nuclear waste glass durability. J Non-Cryst Solids 1984;67:207–23.
[35] Greenberg SA. The depolymerization of silica in sodium hydroxide solution. J Phys Chem 1957;61:960–5.
[36] Bernal SA, Mejía de Gutiérrez R, Pedraza AL, Provis JL. Effect of binder content on the performance of alkali activated slag concretes. Cem Concr Res 2011;41:1–8.
[37] Garcia Lodeiro I, Fernández-Jiménez A, Blanco MT, Palomo A. FTIR study of sol–gel synthesis of cementitious gels: C–S–H and N–A–S–H. J Sol–Gel Sci Technol 2008;45:63–72.
[38] Redden RA. Cement-free binder materials through alkali activation of glass powder as the major source material. M.S. Thesis. Clarkson University; 2010. p. 107.
[39] Giannopoulou I, Panias D. Hydrolytic stability of sodium silicate gels in the presence of aluminum. J Mater Sci 2010;45:5370–7.
[40] Shelby JE. Properties and structure of soda-lime aluminosilicate glasses. J Appl Phys 1989;66(5):1947–50.
[41] Yip CK, Lukey GC, van Deventer JSJ. The coexistence of geopolymeric gel and calcium silicate hydrate at the early stage of alkaline activation. Cem Concr Res 2005;35:1688–97.
[42] Yip CK, van Deventer JSJ. Microanalysis of calcium silicate hydrate gel formed within a geopolymeric binder. J Mater Sci 2003;38:3851–60.
[43] Palacios M, Puertas F. Effect of carbonation on alkali-activated slag paste. J Am Ceramic Soc 2006;89:3211–21.
[44] Ben Haha M, Lothenbach B, Le Saout G, Winnefeld F. Influence of slag chemistry on the hydration of alkali-activated blast furnace slag – Part I: effect of MgO, Cement and Concrete Research. doi: http://dx.doi.org/10.1016/j.cemconres.2011.05.002.
[45] García Lodeiro I, Fernández-Jiménez A, Palomo A, Macphee DE. Effect on fresh C–S–H gels of the simultaneous addition of alkali and aluminium. Cem Concr Res 2010;40:27–32.